doi: 10.53446/actamednicomedia.1846958

Acta Medica Nicomedia

Cilt: 9 (2026), 1-8 / Vol: 9 (2026), 1-8
https://dergipark.org.tr/tr/pub/actamednicomedia

Research Article | Araştırma Makalesi

IN VIVO QUANTITATIVE ULTRASOUND IMAGING ON SKIN FOR NON-INVASIVE CHARACTERIZATION OF BREAST CANCER RELATED LYMPHEDEMA

MEME KANSERİYLE İLİŞKİLİ LENFÖDEMİN İNVAZİV OLMAYAN KARAKTERİZASYONU İÇİN CİLTTE İN VİVO KANTİTATİF ULTRASON GÖRÜNTÜLEME

Irem Demirkan[1*],

[1]Bahcesehir University, Faculty of Engineering and Natural Sciences, Department of Biomedical Engineering, Istanbul, Türkiye.

ABSTRACT

Objective: To study the potential of *in vivo* quantitative ultrasound (QUS) imaging using Rényi Entropy (RE) and attenuation coefficient measurements for non-invasive characterization of skin tissue variations in breast cancer-related lymphedema (BCRL).

Methods: Ultrasound radiofrequency (RF) signals recorded from the skin tissue of the arm in five women with Stage II BCRL and five healthy individuals as controls were analyzed. RE was computed from the RF data to quantify tissue heterogeneity, while the attenuation coefficient was estimated using the spectral-log difference method. Corresponding B-mode images were used for anatomical reference, and statistical comparisons were performed between two groups.

Results: Both RE and attenuation coefficient values were significantly lower in lymphedematous dermis than in healthy skin ($p<0.01$), showing decreased signal complexity and changed acoustic scatterer characteristics associated with lymphatic fluid accumulation. Furthermore, the attenuation coefficients from healthy skin dermis fall into the same range as previously reported values, thus confirming the measurement approach. Spatially quantitative distributions were further demonstrated by parametric mapping of entropy and attenuation, enabling robust differentiation between control subjects and patients with BCRL.

Conclusion: The findings of this study showed that the joint analysis of entropy and attenuation-based quantitative ultrasound metrics is sensitive to edema-related changes in the dermal microstructure of BCRL, detecting changes that are not readily discernible in conventional qualitative B-mode imaging. QUS-derived metrics provide complementary insight into tissue heterogeneity and acoustic energy loss at the microtissue level, whereas B-mode principally offers macroscopic anatomical information.

Keywords: Ultrasound, lymphedema, breast cancer, Rényi entropy, attenuation coefficient

ÖZ

Amaç: Meme kanseriyle ilişkili lenfödemde deri dokusu varyasyonlarını invaziv olmayan bir şekilde karakterize etmek için Rényi Entropisi (RE) ve zayıflama katsayısı ölçümlerini kullanarak *in vivo* kantitatif ultrason görüntülemenin potansiyelini incelemek.

Yöntem: Evre II meme kanseri kaynaklı lenfödemli beş kadın ve kontrol grubu olarak beş sağlıklı bireyin kol deri dokusundan kaydedilen ultrason radyo frekansı (RF) sinyalleri analiz edildi. Doku heterojenliğini ölçmek için RF verilerinden RE hesaplandı, zayıflama katsayısı ise spektral-logaritmik fark yöntemi kullanılarak tahmin edildi. Anatomik referans için karşılık gelen B-mod görüntüleri kullanıldı ve iki grup arasında istatistiksel karşılaştırmalar yapıldı.

Bulgular: Hem RE hem de zayıflama katsayısı değerleri, lenfödemli dermiste sağlıklı deriye göre anlamlı derecede daha düşüktü ($p<0,01$), bu da lenfatik sıvı birikimiyle ilişkili olarak sinyal karmaşıklığında azalma ve akustik saçıcı özelliklerinde değişiklik olduğunu gösterdi. Ayrıca, sağlıklı deri dermisinden elde edilen zayıflama katsayıları, daha önce bildirilen değerlerle aynı aralığa düşmektedir, bu da ölçüm yaklaşımını doğrulamaktadır. Entropi ve zayıflamanın parametrik haritalanmasıyla mekansal olarak nicel dağılımlar daha da gösterilmiş ve kontrol denekleri ile lenfödemli hastalar arasında sağlam bir ayrım yapılması sağlanmıştır.

Sonuç: Bu çalışmanın bulguları, entropi ve zayıflamaya dayalı nicel ultrason metriklerinin ortak analizinin, lenfödemin dermal mikro yapısındaki ödemle ilgili değişikliklere duyarlı olduğunu ve geleneksel nitel B-mod görüntülemede kolayca ayırt edilemeyen değişiklikleri tespit ettiğini göstermiştir. Nicel ultrason kaynaklı metrikler, doku heterojenliği ve mikro doku düzeyinde akustik enerji kaybı hakkında tamamlayıcı bilgiler sağlarken, B-mod esas olarak makroskopik anatomik bilgiler sunmaktadır.

Anahtar Kelimeler: Ultrason, lenfödem, meme kanseri, Rényi entropisi, zayıflama katsayısı

***Corresponding author/İletişim kurulacak yazar:** Irem Demirkan; Bahcesehir University, Faculty of Engineering and Natural Sciences, Department of Biomedical Engineering, Istanbul, Türkiye.
Phone/Telefon: +90 (532) 427 32 57, **e-mail/e-posta:** irem.demirkan@bau.edu.tr
Submitted/Başvuru: 22.12.2025 • **Accepted/Kabul:** 20.01.2026 • **Published Online/Online Yayın:** 10.03.2026

Introduction

Breast cancer is the second most common cause of mortality in women.[1] There are several therapeutic options for breast cancer patients. Among these, surgery is a must for further diagnosis and treatment in the majority of breast cancer patients.[2] Unfortunately, these options are accompanied by many complications, including infection, hematoma, and cellulitis, with lymphedema being the most prominent, arising from disruption of the normal physiology of the axillary lymphatic vessels.[2,3] One of the probable complications is the progression of lymphedema, which is a chronic and severe disease causing an abnormal accumulation of protein-rich fluid in the interstitial tissue. This gives rise to the formation of edema and changes in skin tissue structure.[4,5]

Four clinical stages (0 – 3) are used to classify the progression and severity of breast cancer-related lymphedema (BCRL). The initial stages (0 – 1) are mainly linked to mild and possibly reversible fluid accumulation that can be reversible with declivous position and night rest.[6] In contrast, progressed stages (2 – 3) are characterized by persistent edema that continually becomes more severe, which is not only due to fluid accumulation. Instead, these stages entail distinguishable structural changes in the epidermis, subcutaneous skin, and underlying skeletal muscle. Previous research has shown significant alterations in the skin and subcutaneous fat regarding layer thickness and tissue composition.[7,8] In clinical settings, staging BCRL is a straightforward subjective evaluation process that includes tissue pitting. The patient is classified into a particular stage if the skin becomes "pitted" after applying finger pressure to the area. Although straightforward, this technique lacks robustness and is unable to reliably detect subsurface skin tissue changes. Thus, there is a requirement to explore more advanced diagnostic techniques for the assessment of lymphedema. There are a variety of diagnostic tools for lymphedema through a combination of clinical evaluation, arm volume measurements, and imaging-based approaches, but no standard diagnostic method yet exists. Among imaging modalities, BCRL has been previously evaluated by Magnetic Resonance Imaging (MRI)[9], Computed Tomography[10] (CT) and ultrasound (US).[12,13] While MRI and CT are capable of revealing structural changes in skin tissue, their high cost and limited availability restrict routine clinical application. US provides several benefits for the diagnosis and longitudinal monitoring of BCRL with its low cost, noninvasiveness, and portable nature. Conventional B-mode ultrasound produces two-dimensional (2D) images, in which tissue echogenicity is shown through grayscale intensity changes. However, B-mode imaging exhibits limited sensitivity in the characterization of affected (lymphedema) and unaffected (healthy) skin. This limitation arises from the fact that B-mode images are constructed from the envelope of radio-frequency RF signals backscattered by the tissue. The RF signals originate from reflections at the interfaces between acoustically distinct macroscopic structures larger than the wavelength and from coherent and incoherent scattering generated by tissue microstructures smaller than the wavelength. The use of the signal envelope in the construction of the B-mode image suppresses the frequency information available in the RF signals. As a result, microstructural tissue characteristics occurring below the spatial resolution of conventional ultrasound imaging cannot be properly detected.[14] Similarly, in BCRL, early non-invasive diagnosis of tissue changes is required to also improve prognosis and guide intervention. This clinical limitation points out the value of dedicated non-invasive diagnostic tools and justifies the development of innovative imaging and characterization techniques. Quantitative ultrasound techniques rely on frequency analysis of raw RF signals to obtain information about scattering structures smaller than the ultrasonic wavelength, thereby overcoming limitations and accessing microstructures that are smaller than the spatial resolution of conventional images. Indeed, RF signals contain information on the heterogeneity, size, concentration, and mechanical properties of the skin, subcutaneous fat, and skeletal muscle of the arm. This may also help the clinicians to stage the severity of lymphedema according to changes in skin tissue morphology.

QUS tissue characterization and imaging offer higher sensitivity and specificity values in comparison to conventional ultrasound when differentiating healthy from pathological tissue, resulting in enhancements in diagnostic ultrasound imaging. Spectral study of the raw backscattered RF signals (spectral-based parameterization of RF signals), as well as the echo amplitude envelope's statistical distribution (characterization of the envelope statistics), is the basis of QUS methods.[14] QUS parameters include backscatter coefficient[15] (BSC), attenuation[16], sound speed[17], backscatter envelope statistics parameter[18] and scatter number densities and sizes.[19,20]

Ultrasound backscatter envelope statistics imaging plays a key role in the group of QUS approaches, including, particularly, information entropy imaging, since this can allow one to characterize local scatterer distribution patterns of a tissue visualized, such as scatterer concentration and organizations.[21-23] Ultrasound information entropy imaging approaches are non-model based, in which entropy is used as a biomarker to investigate signal complexity. Entropy is a function of probability density and therefore is linked to the distribution parameters. Shannon Entropy (SE) has been widely measured to characterize a vast amount of

tissue types, where a probability histogram is frequently used to estimate the entropy metric from local ultrasound backscatter envelopes through the consideration of a discrete probability distribution of each bin.[24-26] Ultrasound SE imaging has also been shown to detect variations in local scatter concentrations, revealing underlying microstructural changes.[25] RE is a generalized form of SE quantifying the randomness of probability distribution by an adjustable order parameter (α) controlling the relative emphasis placed on different parts of the distribution[21,23,27.]

QUS parameters have been increasingly explored for the characterization of skin tissue under various pathological conditions. For instance, in the study of *Fornage* et al.,[28] 20 MHz ultrasonic probe was used to make examinations of 10 healthy volunteers' skin aged between 21-43 years old (men and women) at eight sites (forehead, dorsal forearm, dorsum of the hand and palm, nail of the third finger, lower back, calf, and sole) and to analyze 200 benign and malignant skin lesions (i.e., scar, inflammation, nevus, actinic keratosis and melanoma, and basal cell carcinoma). On the one hand, they reported the inability of a 20 MHz US probe to discriminate between benign and malignant lesions. On the other hand, this scanner allowed us to monitor the regularity or irregularity of margins and to measure skin thickness in accordance with the lesion types non-invasively. Moreover, Cammarota et al.[29] reported US examinations using 7.5, 10, 13, and 20 MHz probes to represent a valid adjunct to clinical assessment in many skin conditions, including neoplasms, inflammatory states, and diseases of unknown origin. This study concluded that high-frequency ultrasound could provide a reliable morphologic representation and thickness information of skin lesions. However, it is not efficient to characterize the nature of the tissue, hence distinguishing between benign and malignant lesions. Among different quantitative ultrasonic parameters that have been measured for skin tissue, measurement of the attenuation coefficient and backscatter coefficient seems particularly promising since both have the potential to classify and differentiate between healthy vs. pathological skin tissues. In the case of QUS imaging for skin tissue, one of the studies in the literature has shown that *in vitro*, both sound speed and attenuation in skin tissue were directly linked to collagen distribution and inversely related to water content.[30] Furthermore, Moran et al.[31] measured sound speed, attenuation, and backscatter coefficients from freshly excised human skin, obtained from two cadavers' upper and lower back, chest, and abdomen body regions, between 20 to 30 MHz. The average attenuation coefficients obtained for whole skin were found in agreement with previously published results. They reported no noticeable variation in speed of sound with skin site existing. Introducing the power-law fit model, α_1 refers to the attenuation coefficient value at 1 MHz, and the attenuation coefficient value for the dermis is α_1 = 0.264 ± 0.170 dB/cm, and the power, n=1.69 ± 0.08. The measured backscatter coefficient was on the order of 10^{-6} 1/Sr.cm for the dermis. Moreover, the studies on animal models showed that the attenuation and backscatter coefficients reflect variations as a function of age[32], burn injury[33] and cut healing *in vitro.*[34] Guittet et al. showed that attenuation is useful in detecting variations in skin due to aging *in vivo.*[35] Moreover, Raju et al. reported *in vivo* attenuation and backscatter coefficients from healthy human dermis and subcutaneous fat in the frequency range of 14 to 50 MHz. Attenuation coefficients were found in good agreement with one another.[36] Following that, Raju et al. also showed a decrease in the attenuation coefficient slope and echogenicity at the sites of contact dermatitis.[37] More recently, Omura et al.[38] studied the influences of acoustic and histopathological characteristics on the backscatter properties of *ex vivo* lymphedema (LE) dermis (human tissues negative (n=5) and positive (n=5) with a custom-made scanner with a 14 MHz transducer. Scatterer diameter and acoustic concentration were both derived from the compensated backscatter coefficients by the attenuation values. Both experimental and predicted EACs showed differences (in the 25.7 – 102%) between negative and positive LE cases.

Even though these studies explore optimal methods for *in vitro* and *in vivo* skin measurements and determine the range of values obtained from skin samples, inconsistent ultrasonic measurements are also observed, indicating the effects of system-specific characteristics (i.e., beam diffraction) and underlying variations in the skin structure. There is also a considerable disparity for attenuation measurements across different ultrasound scanners for skin.[33] Moreover, to date, the application of Rényi entropy for characterization of skin tissue and related pathologies has not been explored. In order to close this gap, this study hypothesized that measuring attenuation and Rényi entropy in the skin dermis layer together could yield sensitive and complementary biomarkers for describing skin tissue alterations associated with BCRL. Accordingly, the objective of this study was to measure attenuation coefficient and Rényi entropy in the dermis of breast cancer survivors who had Stage II lymphedema and compare the results with those from a control group.

Methods

Ultrasound Dataset

Attenuation coefficient and Rényi entropy (RE) measurements were conducted using an open-source BCRL ultrasound dataset.[39,40] For this dataset, Alpinion E-Cube 12 system (Bothell, WA, USA) with L3-12H high-

density linear probe with 10 MHz center and 40 MHz sampling frequencies was used for ultrasound imaging. From this dataset, analysis was performed on RF signals corresponding to the third anatomical region known to show pronounced structural changes.[40] The location of the region was defined as 80% of the interval between the syloid process of the fifth digit and olecranon.[39,40] Five women with Stage II BCRL (n=5) were included in the patient group, and five healthy women's (n=5) ultrasound data were included in the Control group.

The patient cohort consisted of 19 women (mean age: 56±14.8 years) with a body mass index (BMI) greater than 24 kg/m^2, enrolled through the McGill Lymphedema Research Program. All women had undergone a surgery and adjuvant treatment for breast cancer more than six years before the data acquisition. In this dataset, the focus was on the Stage II BCRL since Stage I is typically associated with minimal swelling, by limited diagnosed tissue variations compared with normal skin tissue.[39,40]

Attenuation Imaging

In this study, the spectral difference method, based on sliding-window approach, comparing two backscattered RF signals acquired with the focal zone at depths $\boldsymbol{z_1}$ and $z_2(\Delta z = z_2 - z_1 > 0)$ within the skin dermis, was performed by custom script in MATLAB (R2023b, MathWorks, MA, USA). $P_{\text{measured}}(z_1, f)$ and $P_{\text{measured}}(z_2, f)$ are the power spectra of the RF signals windowed around the focal zone (window width: 15λ, with λ the wavelength at central frequency). The attenuation $\alpha(f)$, expressed in dB/mm, was calculated as in Equation 1[21]:

$$\alpha(f) = \frac{1}{4\Delta z} \ln\left(\frac{P_{\text{measured}}(z_1, f)}{P_{\text{measured}}(z_2, f)}\right), \quad (1)$$

in which f is the frequency. The measured attenuation $\alpha(f)$ was then fitted with the power law $\alpha_0 f^b$ to estimate the attenuation coefficient α_0 in $\mathrm{dB}/(\mathrm{mm.\,MHz}^b)$ and the exponent b.

The Rényi Entropy Imaging

In ultrasound imaging, *RE* quantifies the uncertainty of RF signal amplitudes by measuring the randomness of their probability distribution, thus offering information about scatterer density and underlying tissue microstructural heterogeneity.[25,41] The RE of a discrete distribution D with N elements is defined as[27,42-45] :

$$RE_\mu = \frac{1}{1-\mu} \log_b\left(\sum_{i=1}^{N} p_i^\mu\right), \quad (2)$$

where each p_i is the probability computed from the distribution D, and b is the base number, $b > 0$, using $\mu = 2$. Rényi's entropy equals Shannon's when $\mu \to 1$. To measure the entropy, the present study adapted and implemented the block-wise approach for quantitative analysis of BCRL.[46] The analytic signal of the RF data was computed through Hilbert transform, and the magnitude of this representation was taken to produce the two-dimensional (2D) envelope matrix Then, the envelope matrix was divided into distinct blocks using the built-in *blockproc()* function in MATLAB. To compensate for the effect of gain-dependent intensity variations in the estimations, the local envelope data were normalized through their root-mean-square (RMS) amplitude. This block-wise scanning approach generated 2D parametric maps of *RE* estimates across the full field of view, offering a spatial representation of microstructural alterations within the BCRL ultrasound dataset. Analysis windows for each block was defined such that their side length approximately matched one pulse length for entropy-based metrics.[25,41,46] Rényi entropy was also computed by custom script in MATLAB (R2023b, MathWorks, MA, USA) in order to quantify envelope-signal complexity revealing the tissue heterogeneity.

Statistical Analysis

All statistical analyses for attenuation coefficients and REs were performed using custom script in MATLAB (R2023b, MathWorks, MA, USA). Group differences between controls and BCRL patients were investigated using the Mann-Whitney U test. For all experiments, statistical significance was defined as follows: *, *p<0.05*; **, *p<0.01*.

Results

The attenuation coefficient and RE values from RF signals recorded by the dermis layer of five lymphedematous women patients with Stage II and from the same dermis region of five non-lymphedematous control subjects. A comparative statistical analysis proved the RE values were significantly distinguishable between the control group (median of 1.10; interquartile range of 1.07 – 1.44) and the lymphedema patients (median of 0.79; interquartile range of 0.60 – 0.96) (p = 0.007), as shown in Figure 1A. Figure 2 also shows representative information entropy images reflecting clear differences in the spatial arrangement of healthy and lymphedematous dermis layer. In Figure 2A, the skin layers are clearly visible in healthy tissue; yet, lymphatic fluid accumulation associated with lymphedema gives rise to partial separation of these layers. The expanded and more distinguishable dermis beneath the epidermis is demonstrated by a red arrow in Figure 2B.

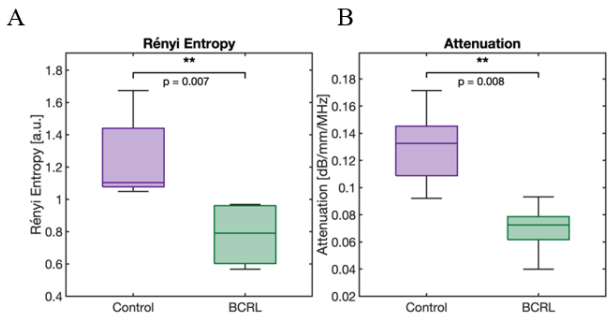

Figure 1. Median values of differences between A) Rényi Entropy (*RE*) and B) Attenuation coefficients in skin dermis of non-lymphedematous and lymphedematous subjects.

A comparative statistical analysis further showed the attenuation coefficient values differed significantly between lymphedema (median of 0.07; interquartile range of 0.06 – 0.08 dB/mm/MHz) and control individuals (median of 0.13; interquartile range of 0.10 – 0.15 dB/mm/MHz) (p = 0.008), as illustrated in Figure 1B. Figure 3 also demonstrates corresponding representative attenuation imaging highlighting low and high attenuating regions for non-lymphedematous and lymphedematous dermal tissue.

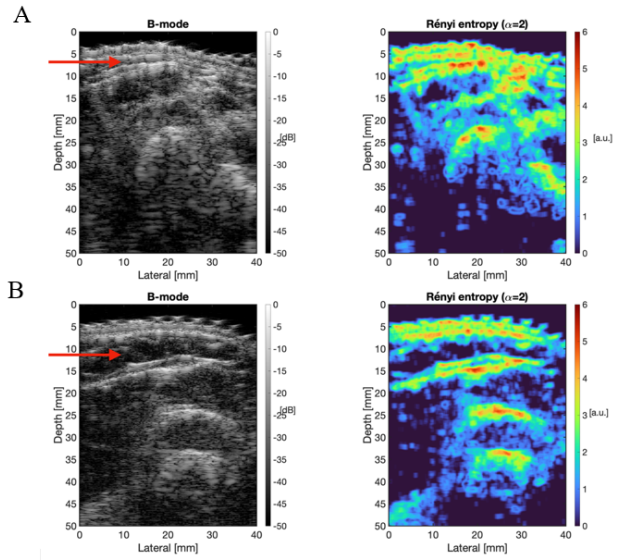

Figure 2. Ultrasound B-mode images and corresponding Rényi entropy maps of (A) non-lymphedematous and (B) lymphedematous subjects.

The attenuation coefficient values measured beneath the epidermis in healthy volunteers were found to fall within a comparable and overlapping range to those reported in the literature.[35,36,47-49] This finding suggested that the acoustic properties of non-affected skin dermis (median of 0.13; interquartile range of 0.10 – 0.15 dB/mm/MHz) were found relatively uniform, which provides indirect evidence for the validity of proposed attenuation coefficient measurement approach in characterization of BCRL skin tissue alterations.

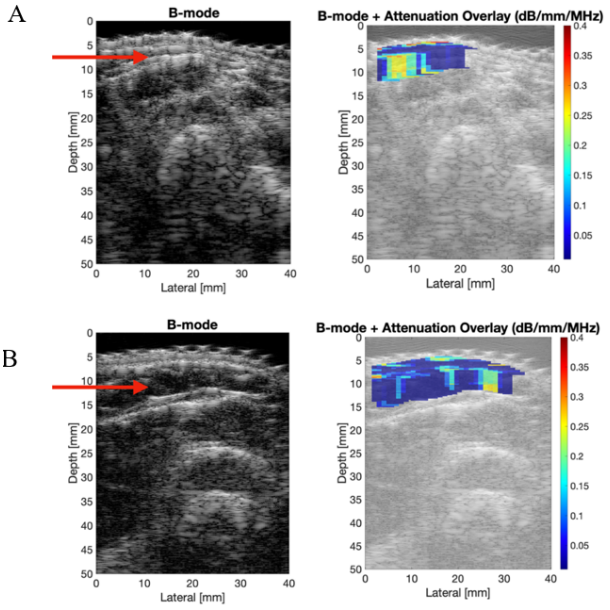

Figure 3. Ultrasound B-mode images and corresponding attenuation maps of (A) non-lymphedematous and (B) lymphedematous subjects.

Discussion

This study explored the possibility of *in vivo* QUS imaging to characterize skin tissue changes between control and BCRL individuals. Specifically, ultrasonic backscatter-derived Rényi entropy and attenuation coefficients were quantified within the dermal (subcutaneous) layer. In addition, conventional B-mode images, from which the QUS metrics were derived, were also demonstrated, showing dermal thickness and echogenicity. Thereby, the B-mode images supported the robustness of the approach proposed in this study. To the best of the author's knowledge, *in vivo* characterization of BCRL dermis has not yet been reported through the combination of non-model-based information entropy and attenuation coefficient measurements. Even though this study was limited to 5 women with diagnosed Stage 2 BCRL, the findings were found promising and showed the potential of RE and attenuation coefficient values to reveal structural differences between healthy and lymphedematous skin tissue.

Entropy refers to a quantitative measure serving as a distribution biomarker of microstructural changes in acoustic scattering media.[41,43,44] Thus, a physical relationship between RE and skin tissue microstructure should be established for translating this approach into clinical applications. In clinical settings, healthy soft tissue can be treated as homogeneous surroundings with a considerable number of randomly distributed scatterers.[36,37,45] Variations in scatterer organization in the scattering medium may serve as a biomarker of the

pathological transformation from normal to abnormal conditions. In abnormal (inhomogeneous) media, high-degree of variance in the scattering cross sections of scatterers give rise to a local variance in the RF signal amplitude, thereby decreasing the width of the probability distribution of the signal. This leads to reduction in the estimated value of entropy. For normal (homogeneous) state, when scatterer density increases, more scatterers within the media directly interact with the ultrasound wave, leading to more complex interference and greater variability in backscattered signal amplitude, which can be quantified as higher entropy values.[25] Accordingly, in the context of BCRL, these principles provide a biologically meaningful explanation for interpretation. Lymphedema is a chronic and severe disease causing an abnormal accumulation of protein-rich fluid in the interstitial tissue. This leads to development of edema and changes in tissue structure, leading to progressive separation of skin tissue layers and disruption of normal dermal and subcutaneous microarchitecture[4,5] Accordingly, such abnormal accumulation of protein-rich fluid in the interstitial tissue may increase the average distance between scatterers, contributing to a more homogeneous scattering environment. As a consequence, since the probability distribution of backscattered amplitudes became narrower and less complex, reduction in entropy values were observed in lymphedematous dermal tissue. This finding was found consistent with a report revealing a decrease in entropy for a more homogeneous breast tissue.[25] Similar pattern was also observed for attenuation coefficient. Attenuation coefficient values for healthy dermal layer (median of 0.13; interquartile range of 0.10 – 0.15 dB/mm/MHz) were comparable to that of a previous study into forearm dermis (median of 0.21; interquartile range of 0.08 – 0.39 dB/mm/MHz).[36] A statistically significant difference was found between healthy subjects and individuals with lymphedema with p = 0.008. This can be attributed to edema-related increases in interstitial fluid content, reducing tissue viscosity and acoustic absorption and giving rise to a more homogeneous surrounding. Thus, water-rich lymphedema dermal layer attenuated ultrasound waves less efficiently than more fibrotic or collagen dense layers, consistent with corresponding decrease in entropy.[34-36] Moreover, the present findings were in contrast with a previous report based on comparison of attenuation values between *ex vivo* lymphedema-negative LE(−) and lymphedema-positive LE(+) tissues.[47] This discrepancy can be explained by methodological differences, including the use of *ex vivo* skin tissues and attenuation estimation methods as well as the clinical stage of lymphedema among the investigated populations.

In conclusion, this study showed the applicability of *in vivo* QUS to non-invasively characterize microstructural changes in skin tissue to better understand breast cancer-related lymphedema. Statistically significant reductions in RE and attenuation coefficient values were observed in lymphedematous skin relative to healthy skin, consistent with edema-related increased microstructural homogeneity and tissue thickening. Although performing the approach on a limited sample size, the findings of this study suggested that combined entropy and attenuation-based QUS metrics may offer objective biomarkers beyond qualitative B-mode imaging. Further investigations on more data are required to make a more definitive conclusion.

Compliance with Ethical Standards

This study utilized a publicly available ultrasound RF dataset. All data were previously collected and anonymized by the original investigators. No new human or animal subjects were involved in this study; therefore, additional ethical approval was not required.

Conflict of Interest

The author declares no conflict of interest.

Author Contribution

ID; Conceptualization, data curation, designed the experiments, formal analysis, investigation, methodology, resources, validation, visualization, writing - original draft preparation, and writing - review and editing.

Financial Disclosure

The author received no financial support.

Acknowledgment

The author would like to thank Gül Gizem KAYA, MD, for her professional support and valuable contributions to the clinical interpretation of the ultrasound images in this study.

References

1. Torre LA, Islami F, Siegel RL, Ward EM, Jemal A. Global cancer in women: burden and trends. *Cancer Epidemiol Biomarkers Prev.* 2017;26(4):444-457. doi:10.1158/1055-9965.EPI-16-0858
2. Josephine SP. Evaluation of lymphedema prevention protocol on quality of life among breast cancer patients with mastectomy. *Asian Pac J Cancer Prev.* 2019;20(10):3077. doi:10.31557/APJCP.2019.20.10.3077
3. Lawenda BD, Mondry TE, Johnstone PAS. Lymphedema: a primer on the identification and management of a chronic condition in oncologic treatment. *CA Cancer J Clin.* 2009;59(1):8-24. doi:10.3322/caac.20001
4. Warren AG, Brorson H, Borud LJ, Slavin SA. Lymphedema: a comprehensive review. *Ann Plast Surg.* 2007;59(4):464-472. doi:10.1097/01.sap.0000257149.42922.7e
5. Mortimer PS. The pathophysiology of lymphedema. *Cancer.* 1998;83(S12B):2798-2802.

doi:10.1002/(SICI)10970142(19981215)83:12B+%3C2798::AIDCNCR28%3E3.0.CO;2-E.
6. Frattolin J, et al. A systematic review and meta-analysis of the incidence of breast cancer-related lymphoedema due to treatment combinations. *medRxiv.* 2025. doi:10.1101/2025.06.11.25329404
7. Pappalardo M, et al. Breast cancer-related lymphedema: recent updates on diagnosis, severity and available treatments. *J Pers Med.* 2021;11(5):402. doi:10.3390/jpm11050402
8. Mellor RH, et al. Dual-frequency ultrasound examination of skin and subcutis thickness in breast cancer-related lymphedema. *Breast J.* 2004;10(6):496-503. doi:10.1111/j.1075-122X.2004.21458.x
9. Ren X, Li L. Magnetic resonance imaging in lymphedema: opportunities, challenges, and future perspectives. *Magn Reson Imaging.* 2025. doi:10.1016/j.mri.2025.110461
10. Akita S, et al. Noninvasive screening test for detecting early stage lymphedema using follow-up computed tomography imaging after cancer treatment and results of treatment with lymphaticovenular anastomosis. *Microsurgery.* 2017;37(8):910-916. doi:10.1002/micr.30188
11. Suehiro K, et al. Significance of ultrasound examination of skin and subcutaneous tissue in secondary lower extremity lymphedema. *Ann Vasc Dis.* 2013;6(2):180-188. doi:10.3400/avd.oa.12.00102
12. Rockson SG. Ultrasonography in the evaluation of breast cancer-related lymphedema. *Lymphat Res Biol.* 2016;14(1):1. doi:10.1089/lrb.2016.28999.sgr
13. Yusof KM, et al. Assessment of potential risk factors and skin ultrasound presentation associated with breast cancer-related lymphedema in long-term breast cancer survivors. *Diagnostics.* 2021;11(8):1303. doi:10.3390/diagnostics11081303
14. Oelze ML, Mamou J. Review of quantitative ultrasound: envelope statistics and backscatter coefficient imaging and contributions to diagnostic ultrasound. *IEEE Trans Ultrason Ferroelectr Freq Control.* 2016;63(2):336-351. doi:10.1109/TUFFC.2015.2513958
15. Yao LX, Zagzebski JA, Madsen EL. Backscatter coefficient measurements using a reference phantom to extract depth-dependent instrumentation factors. *Ultrason Imaging.* 1990;12(1):58-70. doi:10.1016/0161-7346(90)90221-I
16. Kanayama Y, et al. Real-time ultrasound attenuation imaging of diffuse fatty liver disease. *Ultrasound Med Biol.* 2013;39(4):692-705. doi:10.1016/j.ultrasmedbio.2012.10.021
17. Labuda C, et al. Two-dimensional mapping of the ultrasonic attenuation and speed of sound in brain. *Ultrasonics.* 2022;124:106742. doi:10.1016/j.ultras.2022.106742
18. Lizzi FL, et al. Relationship of ultrasonic spectral parameters to features of tissue microstructure. *IEEE Trans Ultrason Ferroelectr Freq Control. 1987*;34(3):319-329. doi:10.1109/T-UFFC.1987.26950
19. Tehrani AKZ, et al. Ultrasound scatterer density classification using convolutional neural networks and patch statistics. *IEEE Trans Ultrason Ferroelectr Freq Control.* 2021;68(8):2697-2706. doi:10.1109/TUFFC.2021.3075912
20. Zhou Z, et al. Scatterer size estimation for ultrasound tissue characterization: a survey. *Measurement.* 2024;225:114046. doi:10.1016/j.measurement.2023.114046
21. Mamou J, Oelze ML, eds. *Quantitative Ultrasound in Soft Tissues.* Dordrecht, Netherlands: Springer; 2013. doi:10.1007/978-94-007-6952-6
22. Tsui PH, et al. Small-window parametric imaging based on information entropy for ultrasound tissue characterization. *Sci Rep.* 2017;7:41004. doi:10.1038/srep41004
23. Vujasic R. Matched reassignment of the ultrasound data of breast lesions. Bachelor's thesis. 2022.
24. Zhou Z, et al. Entropic imaging of cataract lens: an in vitro study. *PLoS One.* 2014;9(4):e96195. doi:10.1371/journal.pone.0096195
25. Tsui PH, et al. Small-window parametric imaging based on information entropy for ultrasound tissue characterization. *Sci Rep.* 2017;7:41004. doi:10.1038/srep41004
26. Fang J, Ting YN, Chen YW. Quantitative assessment of lung ultrasound grayscale images based on Shannon entropy for the detection of pulmonary aeration: an animal study. *J Ultrasound Med.* 2022;41(7):1699-1711. doi:10.1002/jum.15851
27. Rényi A. On measures of entropy and information. In: *Proceedings of the Fourth Berkeley Symposium on Mathematical Statistics and Probability.* Berkeley: University of California Press; 1961:547-562.
28. Fornage BD, McGavran MH, Duvic M, Waldron CA. Imaging of the skin with 20-MHz US. *Radiology.* 1993;189(1):69-76. doi:10.1148/radiology.189.1.8372222
29. Cammarota T, Pinto F, Magliaro A, Sarno A. Current uses of diagnostic high-frequency US in dermatology. *Eur J Radiol.* 1998;27(Suppl):S215-S223. doi:10.1016/S0720-048X(98)00065-5
30. Olerud JE, O'Brien WD Jr, Riederer-Henderson MA, et al. Ultrasonic assessment of skin and wounds with the scanning laser acoustic microscope. *J Invest Dermatol.* 1987;88(5):615-623. doi:10.1111/1523-1747.ep12470221
31. Moran CM, Bush NL, Bamber JC. Ultrasonic propagation properties of excised human skin. *Ultrasound Med Biol.* 1995;21(9):1177-1190. doi:10.1016/0301-5629(95)00049-6
32. Bhagat PK, Kerrick W, Ware RW. Ultrasonic characterization of aging in skin tissue. *Ultrasound Med Biol.* 1980;6(4):369-375. doi:10.1016/0301-5629(80)90006-X
33. Cantrell JH Jr, Goans RE, Roswell RL. Acoustic impedance variations at burn–nonburn interfaces in porcine skin. *J Acoust Soc Am.* 1978;64(3):731-735. doi:10.1121/1.382037
34. Forster FK, Olerud JE, Riederer-Henderson MA, Holmes AW. Ultrasonic assessment of skin and surgical wounds utilizing backscatter acoustic techniques to estimate attenuation. *Ultrasound Med Biol.* 1990;16(1):43-53. doi:10.1016/0301-5629(90)90085-Q
35. Guittet C, Ossant F, Remenieras JP, Pourcelot L, Berson M. High-frequency estimation of the ultrasonic attenuation coefficient slope obtained in human skin: simulation and in vivo results. *Ultrasound Med Biol.*

1999;25(3):421-429. doi:10.1016/S0301-5629(98)00176-8
36. Raju BI, Srinivasan MA. High-frequency ultrasonic attenuation and backscatter coefficients of in vivo normal human dermis and subcutaneous fat. *Ultrasound Med Biol.* 2001;27(11):1543-1556. doi:10.1016/S0301-5629(01)00456-2
37. Raju BI, Swindells KJ, Gonzalez S, Srinivasan MA. Quantitative ultrasonic methods for characterization of skin lesions in vivo. *Ultrasound Med Biol.* 2003;29(6):825-838. doi:10.1016/S0301-5629(03)00009-7
38. Omura M, Yoshida K, Akita S, Yamaguchi T. High-frequency ultrasonic backscatter coefficient analysis considering microscopic acoustic and histopathological properties of lymphedema dermis. *Jpn J Appl Phys.* 2020;59:SKKE15. doi:10.35848/1347-4065/ab86da
39. Goudarzi S, et al. Segmentation of arm ultrasound images in breast cancer-related lymphedema: a database and deep learning algorithm. *IEEE Trans Biomed Eng.* 2023;70(9):2552-2563. doi:10.1109/TBME.2023.3253646
40. Hashemi HS, et al. Assessment of mechanical properties of tissue in breast cancer-related lymphedema using ultrasound elastography. *IEEE Trans Ultrason Ferroelectr Freq Control.* 2019;66(3):541-550. doi:10.1109/TUFFC.2018.2876056
41. Christensen AM, Rosado-Mendez IM, Hall TJ. A systematized review of quantitative ultrasound based on first-order speckle statistics. *IEEE Trans Ultrason Ferroelectr Freq Control.* 2024;71(7):872-886.
42. Suehiro K, et al. Skin and subcutaneous tissue ultrasonography features in breast cancer-related lymphedema. Ann Vasc Dis. 2016;9(4):312-316. doi:10.3400/avd.oa.16-00086
43. Shannon CE. A mathematical theory of communication. *Bell Syst Tech J.* 1948;27(3):379-423.
44. Hughes MS. Analysis of ultrasonic waveforms using Shannon entropy. In: *IEEE 1992 Ultrasonics Symposium Proceedings.* IEEE; 1992:1205-1209. doi:10.1109/ULTSYM.1992.275884
45. Smolíková R, Wachowiak MP, Zurada JM. An information-theoretic approach to estimating ultrasound backscatter characteristics. *Comput Biol Med.* 2004;34(4):355-370. doi:10.1016/S0010-4825(03)00072-6
46. Gao R, et al. Ultrasound normalized cumulative residual entropy imaging: theory, methodology, and application. Comput Methods Programs Biomed. 2024;256:108374. doi:10.1016/j.cmpb.2024.108374
47. Omura M, et al. Frequency dependence of attenuation and backscatter coefficient of ex vivo human lymphedema dermis. *J Med Ultrason.* 2020;47(1):25-34. doi:10.1007/s10396-019-00973-z
48. Van den Aarssen M, Verhoef WA, Thijssen JM. Influence of absorbing and scattering media on the propagation of ultrasound. *J Acoust Soc Am.* 1989;85(2):567-575. doi:10.1121/1.397580
49. Frem HS, Giblin RA. The choice of ultrasound frequency for skin blood flow investigation. *Bioeng Skin.* 1985;1(3):193-205.